

Neutron stars and nucleons: Are they so different?

Based on [C.L., Eur. Phys. J. C78 (2018)]
[C.L., Moutarde, Trawinski, *in preparation*]

Cédric Lorcé



October 9, La Grande Motte, France

Outline

- 1. Nucleon structure**
- 2. Energy-momentum tensor**
- 3. Mass decompositions**
- 4. 3D distributions in Breit frame**
- 5. Comparison with neutron stars**
- 6. Summary**

Origin of mass and spin?

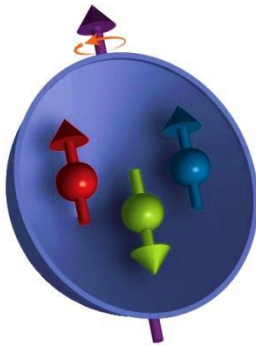
Non-relativistic picture
dominated by **constituents**

Mass

Spin

Until
~ 1980

Spectroscopy



$$M_N \sim \sum_Q M_Q + E_{\text{binding}}$$

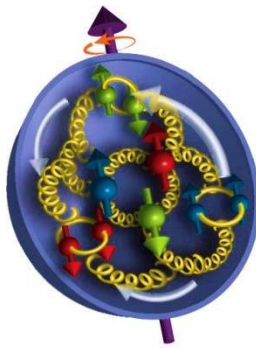
~ 102 % ~ - 2 %

$$J_z^N \sim \sum_Q S_z^Q$$

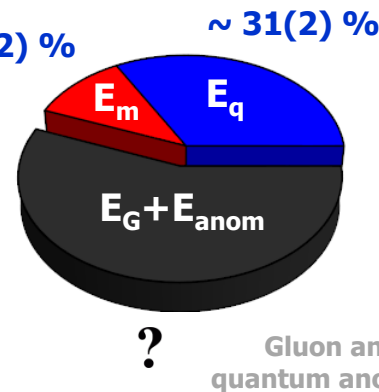
~ 100 %

Relativistic picture
dominated by **dynamics**

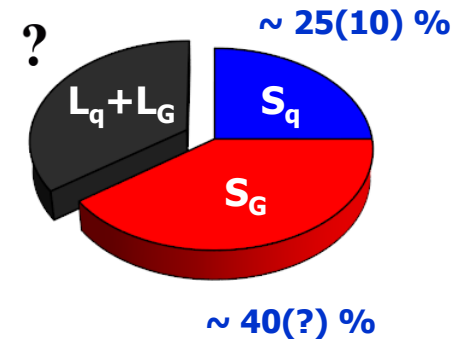
Now
High-energy
scattering



Higgs
mechanism
~ 13(2) %



Orbital angular
momentum



Hot news

PREPUBLICATION COPY—SUBJECT TO FURTHER EDITORIAL CORRECTION

**An Assessment of
U.S.-Based Electron-Ion Collider Science**

Committee on U.S.-Based Electron-Ion Collider Science Assessment
Board on Physics and Astronomy
Division on Engineering and Physical Sciences
A Consensus Study Report of
The National Academies of
SCIENCES · ENGINEERING · MEDICINE

THE NATIONAL ACADEMIES PRESS
Washington, DC
www.nap.edu

PREPUBLICATION COPY—SUBJECT TO FURTHER EDITORIAL CORRECTION

that Hearing from experts on the science that an EIC would be able to carry out, the committee finds

Finding 1: An EIC can uniquely address three profound questions about nucleons—neutrons and protons—and how they are assembled to form the nuclei of atoms:

- How does the mass of the nucleon arise?
- How does the spin of the nucleon arise?
- What are the emergent properties of dense systems of gluons?

Summary extract from a report by the **U.S. National Academy of Sciences** on the science of U.S.-based Electron-Ion Collider (July 24, 2018)

First experimental extraction of the pressure distribution inside the proton
[Burkert, Elouadrhiri, Girod, *Nature* 557 (2018)]



Soon brand new data from
JLab 12GeV and COMPASS II!

LETTER

<https://doi.org/10.1038/s41586-018-0040-z>

The pressure distribution inside the proton

V. D. Burkert¹*, L. Elouadrhiri¹ & F. X. Girod¹

The proton, one of the components of atomic nuclei, is composed of fundamental particles called quarks and gluons. Gluons are the carriers of the force that binds quarks together, and free quarks cannot exist in isolation—that is, they are confined within hadrons in which they reside. The origin of quark confinement is one of the most important questions in modern physics, and it is at the core of understanding the emergent properties of dense systems of gluons.

The pressure, one of the components of atomic nuclei, is composed of fundamental particles called quarks and gluons. Gluons are the carriers of the force that binds quarks together, and free quarks cannot exist in isolation—that is, they are confined within hadrons in which they reside. The origin of quark confinement is one of the most important questions in modern physics, and it is at the core of understanding the emergent properties of dense systems of gluons.

We then define the complex CFF, \mathcal{F}_2 , which is directly related to the experimental observables describing the DVCS process, that is, the differential cross-section and the beam spin asymmetry.

The real and imaginary parts of \mathcal{F}_2 can be related through a dispersion relation^{18,19} at fixed t , where the term $D(t)$, or D -term, appears as a subtraction term²⁰.

We derive $d_1(t)$ from the expansion of $D(t)$ in the Gegenbauer polynomials C_n of the momentum transfer to the struck quark.

We apply fits to the data and extract $D(t)$ and $d_1(t)$.

We determine the pressure distribution from the relation $P(r) = -\frac{1}{4\pi} \nabla^2 \int d^3x' \mathcal{L}(D(x) = M(x)) = \frac{1}{2\pi} \int_0^\infty \frac{d^2k_\perp}{k_\perp^2} \mathcal{L}(D(k_\perp^2))$.

emitted high-energy photons, which are scattered off quarks, and the scattered electrons and recoil protons. We find a strong repulsive pressure near the center of the proton (up to 6 femtonewtons) and a binding pressure at greater distances. The average peak pressure near the center is about 10^8 pascals, which exceeds the pressure estimated for the most densely packed known objects in the Universe, neutron stars²¹. This work opens up a new area of research on the fundamental gravitational properties of protons, neutrons and nuclei, which can provide access to their physical radii, the internal shear forces acting on the quarks and their pressure distributions.

The basic mechanical properties of the proton are encoded in the gravitational form factors (GFFs) of the energy-momentum tensor²². Graviton-proton scattering is the only known process that can be used to directly measure these form factors²³, whereas generalized parton distributions^{24,25} enable indirect access to the basic mechanical properties of the proton²⁶.

A direct determination of the quark pressure distribution in the proton (Fig. 1) requires measurements of the proton matrix element of the energy-momentum tensor²⁷. This matrix element contains three scalar GFFs that depend on the four-momentum transfer to the proton. One of these GFFs, $d_1(t)$, encodes the shear force and pressure distribution on the quarks in the proton, and the other two, $M(t)$ and $F(t)$, encode the mass and angular momentum distributions. Experimental information on these form factors is essential to gain insight into the dynamics of the fundamental constituents of the proton. The framework of generalized parton distributions (GPDs)²⁸ has provided a way to obtain information on $d_1(t)$ from experiments. The most effective way to access GPDs experimentally is deeply virtual Compton scattering (DVCS)²⁹, where high-energy electrons (e) are scattered from the protons (p) in liquid hydrogen as $e p \rightarrow e' p'$, and the scattered electron (e'), proton (p') and photon (γ) are detected in coincidence. In this process, the quark structure is probed with high-energy virtual photons that are exchanged between the scattered electron and the proton, and the emitted (real) photon controls the momentum transfer t to the proton, while leaving the proton intact. Recently, methods have been developed to extract information about the GFFs and the related Compton form factors (CFFs) from DVCS data³⁰.

To determine the pressure distribution in the proton from the experimental data, we follow the steps that we briefly describe here. We note that the GPDs, CFFs and GFFs apply only to quarks, not to gluons.

(1) We begin with the sum rules that relate the Mellin moments of the GPDs to the GFFs³¹.

(2) We then define the complex CFF, \mathcal{F}_2 , which is directly related to the experimental observables describing the DVCS process, that is, the differential cross-section and the beam spin asymmetry.

(3) The real and imaginary parts of \mathcal{F}_2 can be related through a dispersion relation^{18,19} at fixed t , where the term $D(t)$, or D -term, appears as a subtraction term²⁰.

(4) We derive $d_1(t)$ from the expansion of $D(t)$ in the Gegenbauer polynomials C_n of the momentum transfer to the struck quark.

(5) We apply fits to the data and extract $D(t)$ and $d_1(t)$.

(6) We determine the pressure distribution from the relation $P(r) = -\frac{1}{4\pi} \nabla^2 \int d^3x' \mathcal{L}(D(x) = M(x)) = \frac{1}{2\pi} \int_0^\infty \frac{d^2k_\perp}{k_\perp^2} \mathcal{L}(D(k_\perp^2))$.

10x the pressure @ center of neutron stars!

$\int d^3x' \mathcal{L}(D(x) = M(x)) = \frac{1}{2\pi} \int_0^\infty \frac{d^2k_\perp}{k_\perp^2} \mathcal{L}(D(k_\perp^2))$

Fig. 1 Radial pressure distribution in the proton. The graph shows the pressure distribution $P(r)$ (in GeV/fm³) versus the radial distance r (in fm) from the centre of the proton. The thick black line corresponds to the pressure extracted from the D-term parameters fitted to published data³⁰ measured at a GeV. The corresponding estimated uncertainties are displayed as the light green shaded area shown. The blue area represents the uncertainties from all the data that were available before the COMPASS experiment, and the red shaded area shows projected results from future experiments at 12 GeV that will be performed with the upgraded experimental apparatus³². Uncertainties represent one standard deviation.

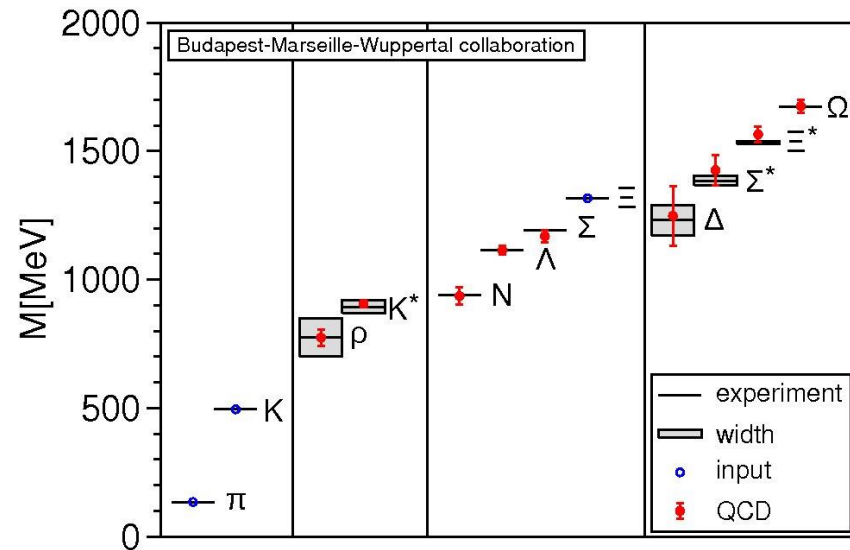
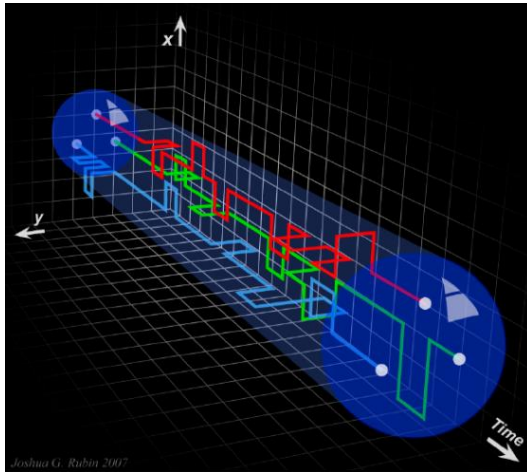
Thomas Jefferson National Accelerator Facility, Newport News, VA, USA. *e-mail: burkert@jlab.org

396 | NATURE | VOL 557 | 17 MAY 2018

© 2018 Macmillan Publishers Limited, part of Springer Nature. All rights reserved.

Lattice QCD

Ab initio mass calculation based on Euclidean space-time correlators $\sim \sum_n e^{-E_n \tau}$



[Dürr *et al.* (2008)]

Unfortunately, little insight on where mass comes from ...

Energy-momentum tensor (EMT)

Mass, spin and pressure all encoded in

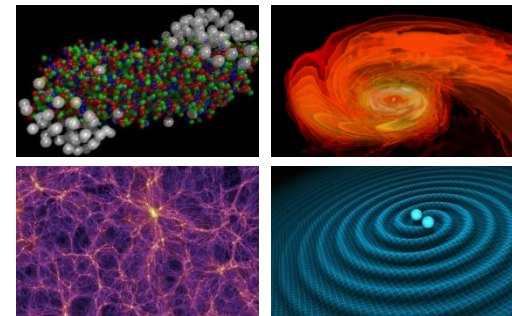
$$T^{\mu\nu} = \begin{bmatrix} \text{Energy density} & & & \\ T^{00} & T^{01} & T^{02} & T^{03} \\ T^{10} & T^{11} & T^{12} & T^{13} \\ T^{20} & T^{21} & T^{22} & T^{23} \\ T^{30} & T^{31} & T^{32} & T^{33} \\ & \text{Energy flux} & \text{Momentum flux} & \end{bmatrix}$$

Shear stress

Normal stress (pressure)

Key concept for

- Nucleon mechanical properties
- Quark-gluon plasma
- Relativistic hydrodynamics
- Stellar structure and dynamics
- Cosmology
- Gravitational waves
- Modified theories of gravitation
- ...



Gravitational form factors (GFFs)

Matrix elements

$$P = \frac{p' + p}{2}, \quad \Delta = p' - p, \quad t = \Delta^2$$

[Kobzarev, Okun (1962)]

[Pagels (1966)]

[Ji (1996)]

[Bakker, Leader, Trueman (2004)]

[Leader, C.L. (2014)]

$$\langle p', s' | T^{\mu\nu}(0) | p, s \rangle =$$

$$\bar{u}(p', s') \left[\frac{P^\mu P^\nu}{M} A(t) + \frac{P^{\{\mu i \sigma^\nu\} \lambda} \Delta_\lambda}{4M} (A + B)(t) + \frac{\Delta^\mu \Delta^\nu - g^{\mu\nu} \Delta^2}{M} C(t) \right.$$

$$\left. + \boxed{M g^{\mu\nu} \bar{C}(t)} + \boxed{\frac{P^{[\mu i \sigma^\nu] \lambda} \Delta_\lambda}{4M} D(t)} \right] u(p, s)$$

Non-conservation

Intrinsic spin

Mass-shell conditions

$$p'^2 = p^2 = M^2$$



$$P^2 = M^2 - \frac{t}{4},$$

Timelike



« frame »



$$P \cdot \Delta = 0$$



Spacelike



« position »

Quantum chromodynamics (QCD)

Classical QCD energy-momentum tensor

$$T^{\mu\nu} = \bar{\psi} \gamma^\mu \frac{i}{2} \overleftrightarrow{D}^\nu \psi - G^{a\mu\alpha} G^{a\nu}{}_\alpha + \frac{1}{4} \eta^{\mu\nu} G^2$$

Renormalized trace of the QCD EMT

$$T^\mu{}_\mu = \underbrace{\frac{\beta(g)}{2g} G^2}_{\text{Trace anomaly}} + (1 + \gamma_m) \bar{\psi} m \psi$$

↑
Quark mass matrix

[Crewther (1972)]
 [Chanowitz, Ellis (1972)]
 [Nielsen (1975)]
 [Adler, Collins, Duncan (1977)]
 [Collins, Duncan, Joglekar (1977)]
 [Nielsen (1977)]

Poincaré invariance

$$\partial_\mu T^{\mu\nu} = 0 \quad \Rightarrow \quad \sum_{i=q,g} A_i(0) = 1, \quad \sum_{i=q,g} \bar{C}_i(t) = 0$$

$$\underbrace{\partial_\mu J^{\mu\alpha\beta}}_{x^\alpha T^{\mu\beta} - x^\beta T^{\mu\alpha} + S^{\mu\alpha\beta}} = 0 \quad \Rightarrow \quad \sum_{i=q,g} B_i(0) = 0, \quad D_q(t) = -G_A^q(t)$$

[Kobzarev, Okun (1962)]
 [Teryaev (1999)]
 [Brodsky, Hwang, Ma, Schmidt (2001)]
 [Leader, C.L. (2014)]
 [Teryaev (2016)]
 [Lowdon, Chiu, Brodsky (2017)]

Textbook decomposition

Forward matrix element

$$\langle P|T^{\mu\nu}(0)|P\rangle = 2P^\mu P^\nu$$

$$\langle P'|P\rangle = 2P^0 (2\pi)^3 \delta^{(3)}(\vec{P}' - \vec{P})$$

Trace decomposition

$$\begin{aligned} 2M^2 &= \langle P|T^\mu{}_\mu(0)|P\rangle \\ &= \underbrace{\langle P|\frac{\beta(g)}{2g} G^2|P\rangle}_{\sim 89\%} + \underbrace{\langle P|(1 + \gamma_m)\bar{\psi}m\psi|P\rangle}_{\sim 11\%} \end{aligned}$$

[Shifman, Vainshtein, Zakharov (1978)]
[Luke, Manohar, Savage (1992)]
[Donoghue, Golowich, Holstein (1992)]
[Kharzeev (1996)]
[Bressani, Wiedner, Filippi (2005)]
[Roberts (2017)]
[Krein, Thomas, Tsushima (2017)]



Manifestly covariant



Compatible with Gell-Mann–Oakes–Renner formula for pion



Depends on state normalization



No spatial extension



No clear relation to energy

Ji's decomposition

[Ji (1995)]

Separation of quark and gluon contributions

$$T^{\mu\nu} = \bar{T}^{\mu\nu} + \hat{T}^{\mu\nu} \quad \bar{T}^{\mu\nu} = \bar{T}_q^{\mu\nu} + \bar{T}_g^{\mu\nu} \quad \hat{T}^{\mu\nu} = \hat{T}_m^{\mu\nu} + \hat{T}_a^{\mu\nu}$$

Traceless Pure trace

Forward matrix elements

$$\begin{aligned} \langle P | \bar{T}_i^{\mu\nu}(0) | P \rangle &= 2 \left(P^\mu P^\nu - \frac{1}{4} \eta^{\mu\nu} M^2 \right) A_i(0) \\ \langle P | \hat{T}_i^{\mu\nu}(0) | P \rangle &= \frac{1}{2} \eta^{\mu\nu} M^2 [A_i(0) + 4\bar{C}_i(0)] \end{aligned} \quad \langle O \rangle = \frac{\langle P | \int d^3r O(r) | P \rangle}{\langle P | P \rangle}$$

Ji's decomposition

[Gao *et al.* (2015)]

$$M = \underbrace{M_q}_{\sim 31\%} + \underbrace{M_g}_{\sim 34\%} + \underbrace{M_m}_{\sim 13\%} + \underbrace{M_a}_{\sim 22\%}$$

$\mu = 2 \text{ GeV}$

$$\begin{aligned} M_q &= \langle \bar{T}_q^{00} \rangle |_{\vec{P}=\vec{0}} - \frac{3}{1+\gamma_m} \langle \hat{T}_m^{00} \rangle |_{\vec{P}=\vec{0}} \\ M_g &= \langle \bar{T}_g^{00} \rangle |_{\vec{P}=\vec{0}} \\ M_m &= \frac{4+\gamma_m}{1+\gamma_m} \langle \hat{T}_m^{00} \rangle |_{\vec{P}=\vec{0}} \\ M_a &= \langle \hat{T}_a^{00} \rangle |_{\vec{P}=\vec{0}} \end{aligned}$$



Proper normalization



Clear relation to energy distribution



Scale-dependent interpretation in the rest frame



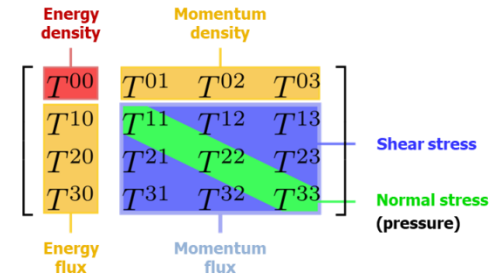
Pressure effects not taken into account

New decomposition

[C.L. (2017)]

Forward matrix element

$$\langle P | T_i^{\mu\nu}(0) | P \rangle = 2P^\mu P^\nu A_i(0) + 2M^2 \eta^{\mu\nu} \bar{C}_i(0)$$



Analogy with relativistic hydrodynamics

Perfect fluid element

$$\Theta_i^{\mu\nu} = (\varepsilon_i + p_i) u^\mu u^\nu - p_i \eta^{\mu\nu}$$



Four-velocity

$$u^\mu = P^\mu / M$$

Energy density

$$\varepsilon_i = [A_i(0) + \bar{C}_i(0)] \frac{M}{V}$$

Isotropic pressure

$$p_i = -\bar{C}_i(0) \frac{M}{V}$$

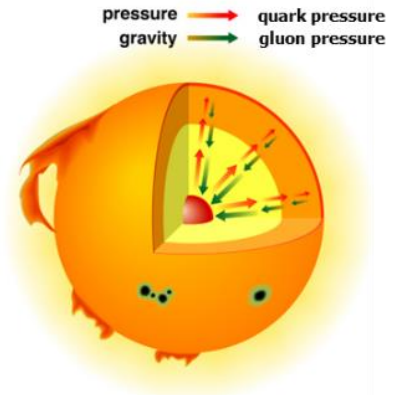
Nucleon mass decomposition $U_i = \varepsilon_i V$

$$M = \underbrace{U_q}_{\sim 44\%} + \underbrace{U_g}_{\sim 56\%}$$

$\mu = 2 \text{ GeV}$

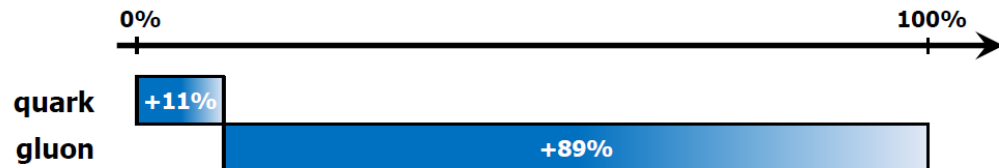
$$p_q = -p_g$$

$\sim 11\%$

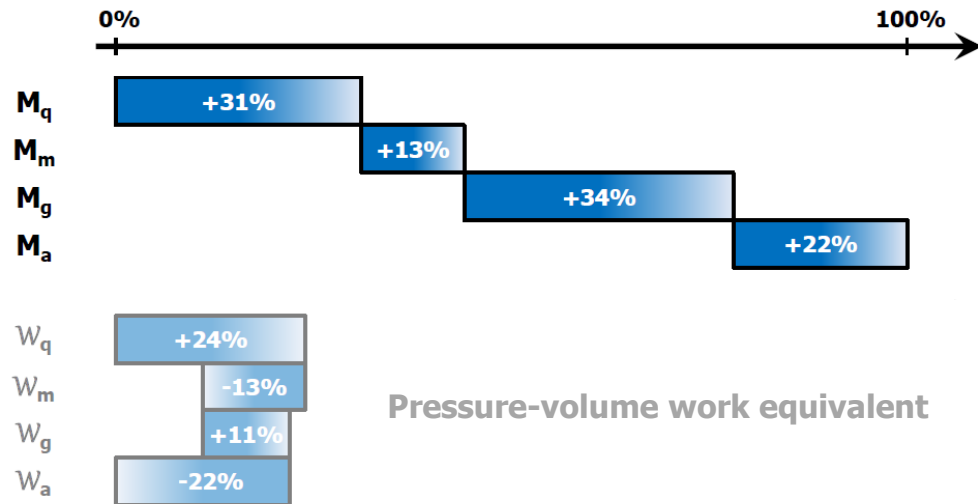


In short

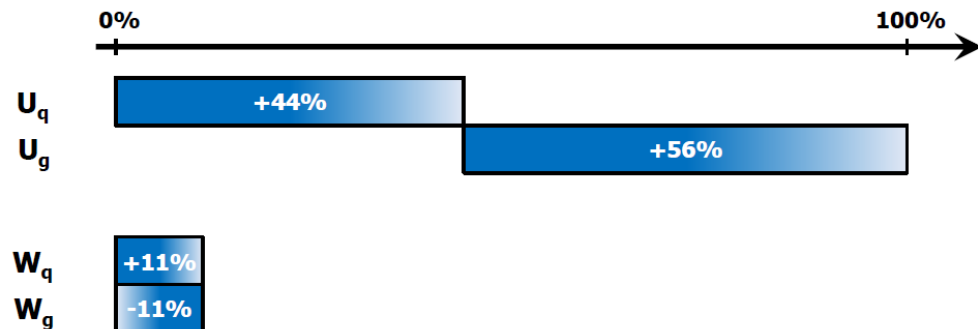
Trace decomposition



Ji's decomposition



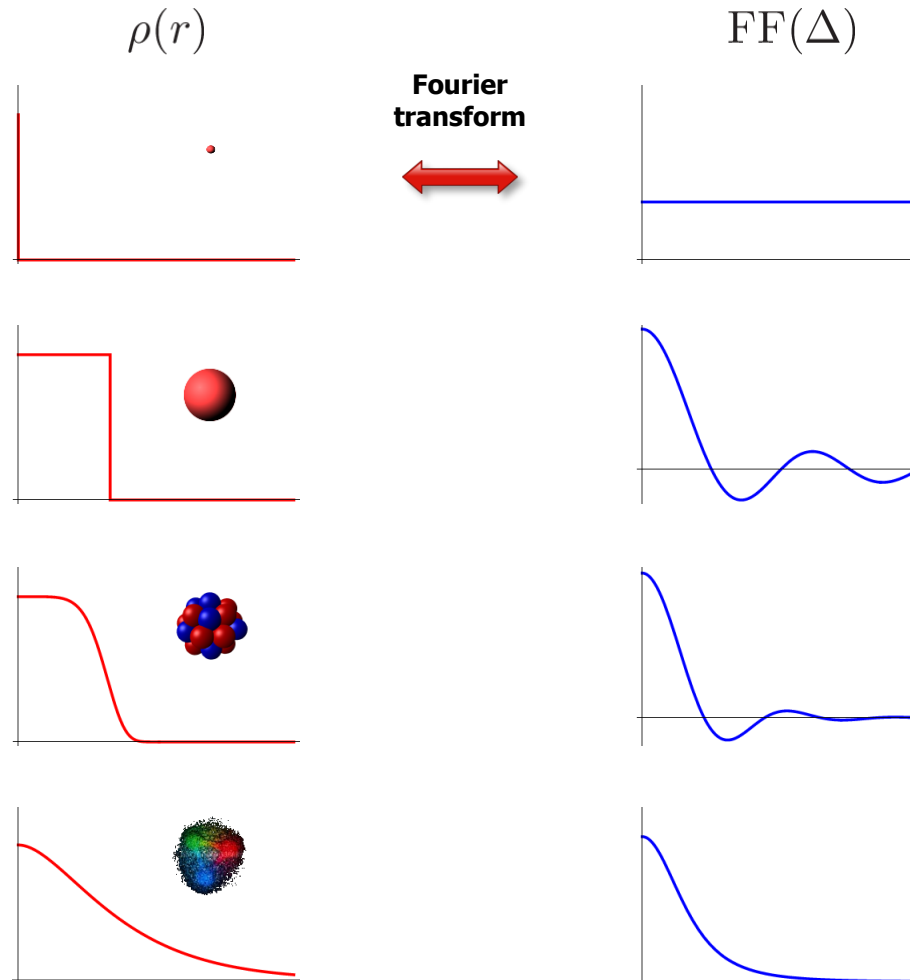
New decomposition



Spatial information

Charge distribution

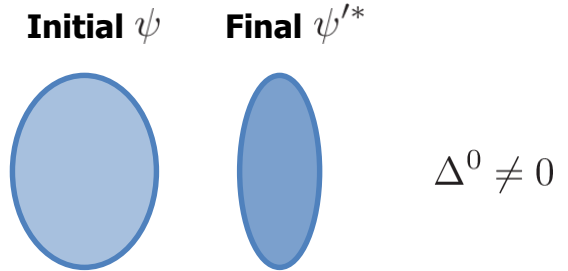
Electric form factor



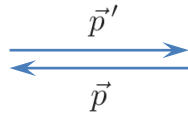
3D distribution in Breit frame

Lorentz factors

$$p^0 = \gamma M, \quad p'^0 = \gamma' M$$



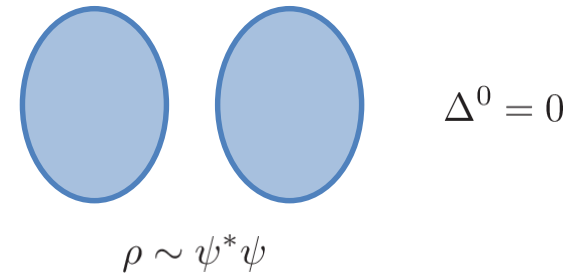
Breit frame



$$\vec{P} = \vec{0}$$



$$\Delta^0 = \frac{\vec{P} \cdot \vec{\Delta}}{P^0} = 0$$



3D distribution

$$\mathcal{T}_i^{\mu\nu}(\vec{r}) = \int \frac{d^3\Delta}{(2\pi)^3 2P^0} e^{-i\vec{\Delta} \cdot \vec{r}} \langle \frac{\vec{\Delta}}{2} | T_i^{\mu\nu}(0) | -\frac{\vec{\Delta}}{2} \rangle$$

Anisotropic medium

[Polyakov (2003)]
 [Goetze *et al.* (2007)]
 [Polyakov, Schweitzer (2018)]
 [C.L., Moutarde, Trawinski, *in preparation*]

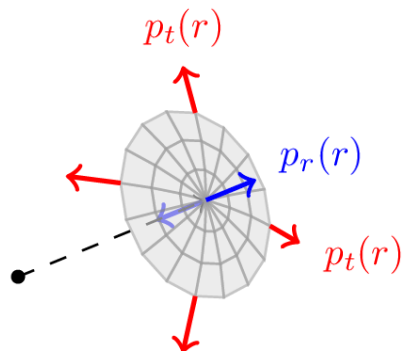
Breit frame amplitude $t = -\vec{\Delta}^2$

$$\frac{\langle \frac{\vec{\Delta}}{2} | T_i^{\mu\nu}(0) | -\frac{\vec{\Delta}}{2} \rangle}{2P^0} = M \left\{ \eta^{\mu 0} \eta^{\nu 0} \left[A_i(t) + \frac{t}{4M^2} B_i(t) \right] + \eta^{\mu\nu} \left[\bar{C}_i(t) - \frac{t}{M^2} C_i(t) \right] + \frac{\Delta^\mu \Delta^\nu}{M^2} C_i(t) \right\}$$

Analogy with relativistic hydrodynamics $r = |\vec{r}|$

Anisotropic fluid

$$\Theta_i^{\mu\nu}(\vec{r}) = [\varepsilon_i(r) + p_{t,i}(r)] u^\mu u^\nu - p_{t,i}(r) \eta^{\mu\nu} + [p_{r,i}(r) - p_{t,i}(r)] \frac{r^\mu r^\nu}{r^2}$$



Isotropic pressure

$$p_i(r) = \frac{p_{r,i}(r) + 2p_{t,i}(r)}{3}$$

Pressure anisotropy

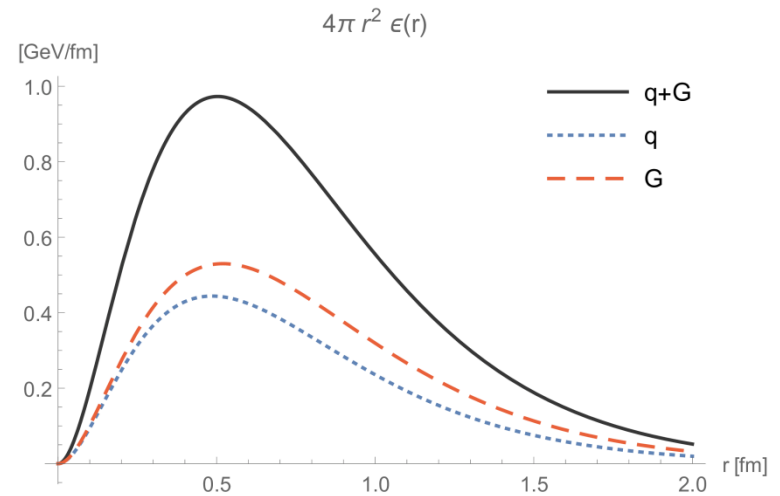
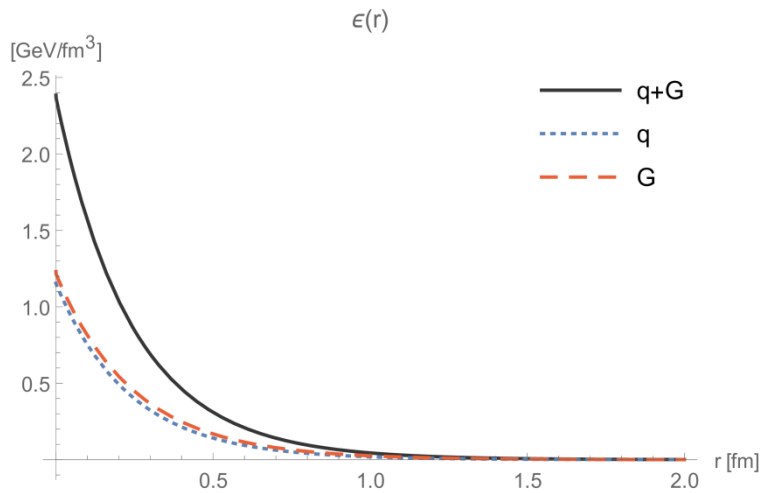
$$s_i(r) = p_{r,i}(r) - p_{t,i}(r)$$

Energy distribution

[C.L., Moutarde, Trawinski, *in preparation*]

Multipole model for the GFFs

$$F(t) = \frac{F(0)}{(1 + t/\Lambda^2)^n}$$

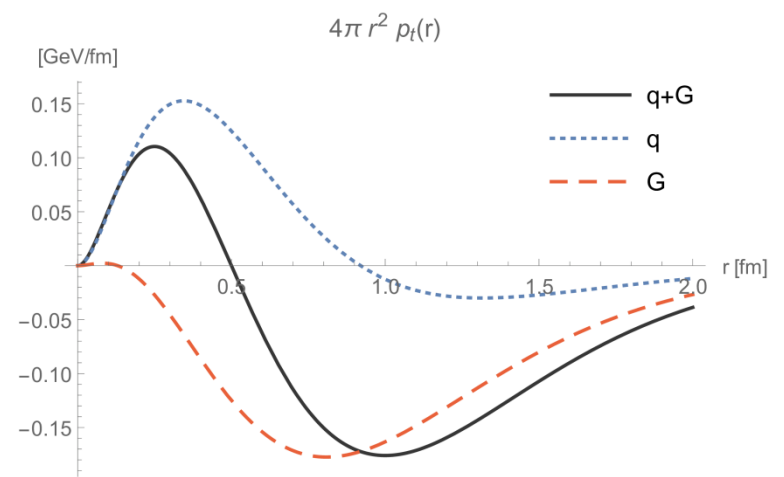
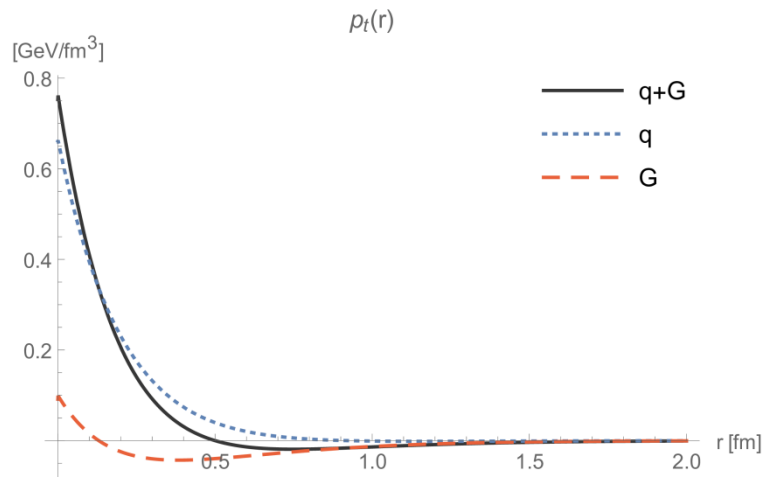
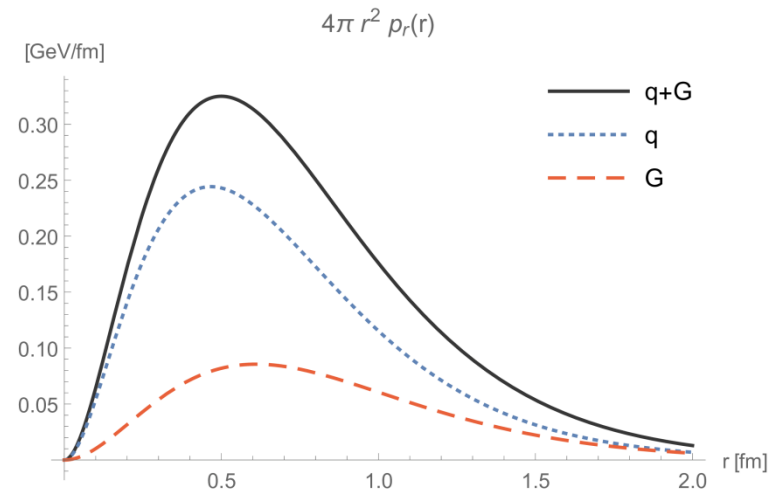
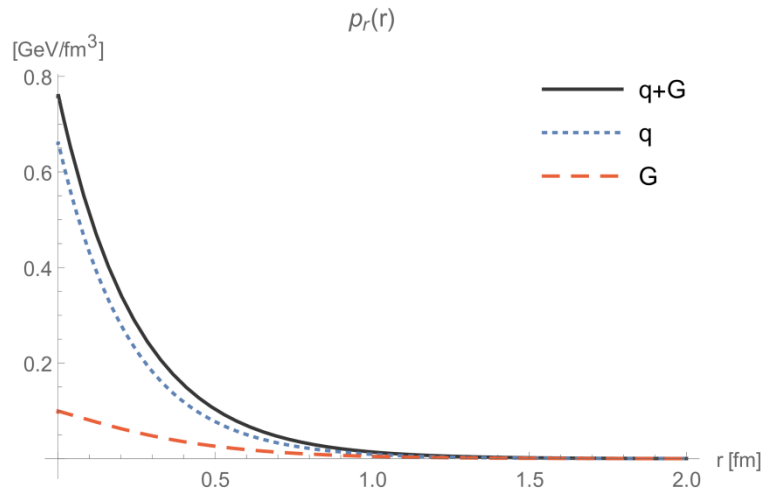


$$\sqrt{\langle r^2 \rangle_M} = 0.91 \text{ fm}$$

$$\sqrt{\langle r^2 \rangle_Q} = 0.84 - 0.88 \text{ fm}$$

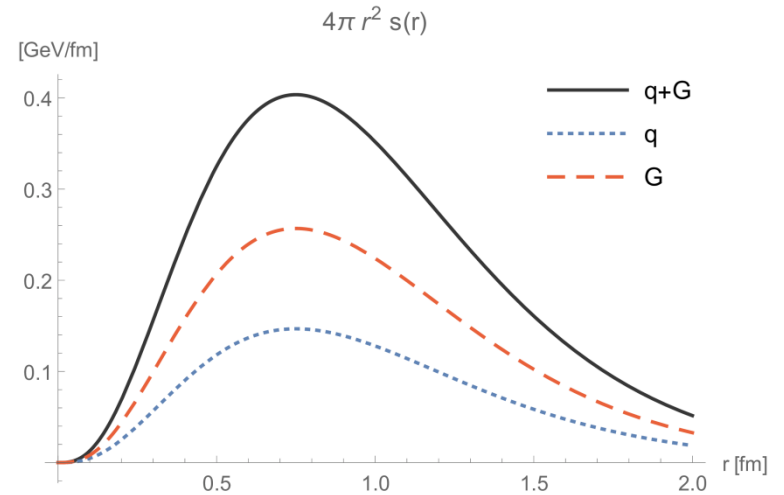
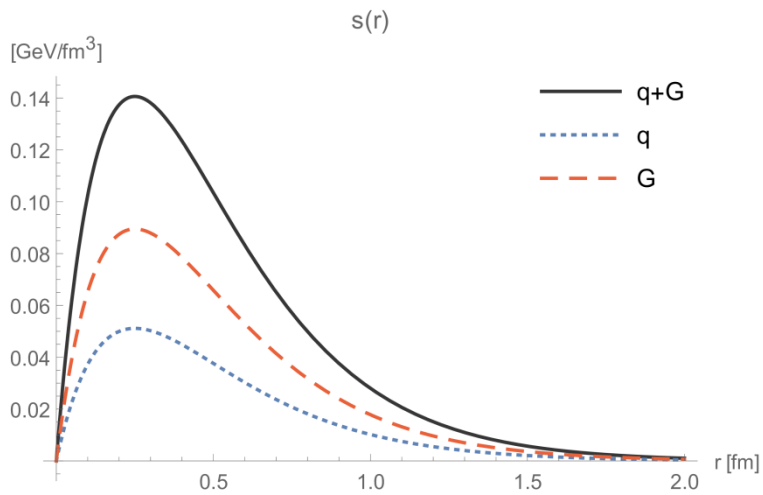
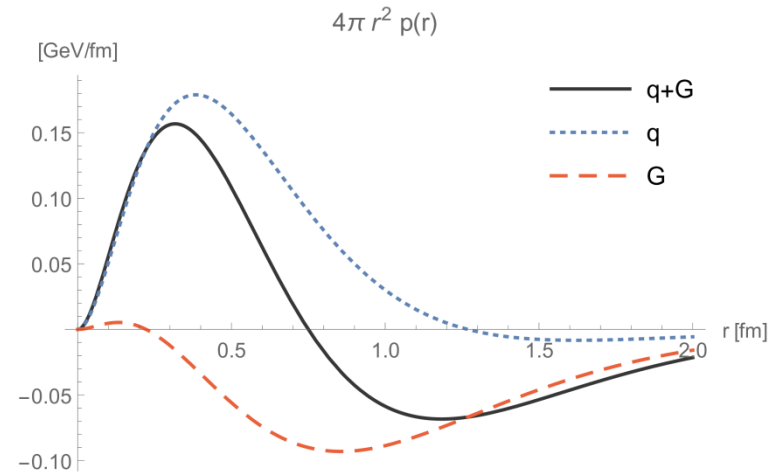
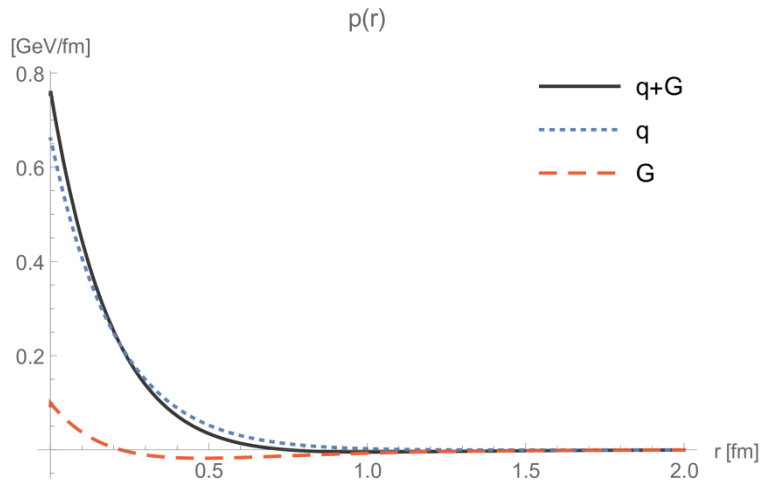
Pressure distribution

[C.L., Moutarde, Trawinski, *in preparation*]



Pressure distribution

[C.L., Moutarde, Trawinski, *in preparation*]



Hydrostatic equilibrium

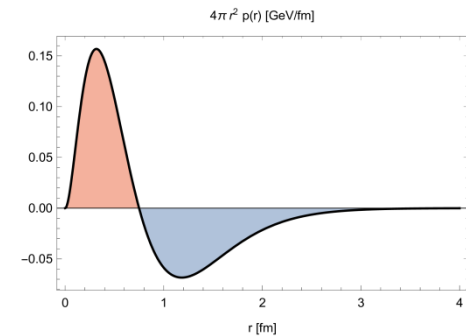
[Polyakov (2003)]
 [Goetze *et al.* (2007)]
 [Polyakov, Schweitzer (2018)]
 [C.L., Moutarde, Trawinski, *in preparation*]

$$\nabla^i \mathcal{T}^{ij}(\vec{r}) = 0 \quad \Rightarrow \quad \frac{dp_r(r)}{dr} = -\frac{2s(r)}{r}$$

von Laue relation

[von Laue (1911)]

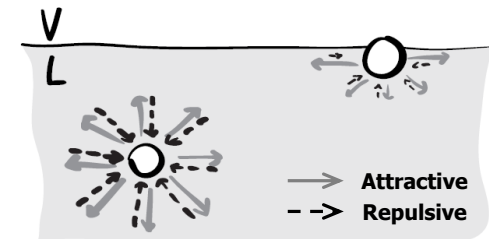
$$\int_0^\infty dr r^2 p(r) = 0$$



Surface tension

[Bakker (1928)]
 [Kirkwood, Buff (1949)]
 [Marchand *et al.* (2011)]

$$\gamma = \int dr s(r)$$



Generalized Young-Laplace relation

$$p(0) = 2 \int_0^\infty dr \frac{s(r)}{r}$$

[Thomson (1858)]

$$s(r) \approx \gamma \delta(r - R) \quad \Rightarrow \quad p(0) = \frac{2\gamma}{R}$$

Highest energy densities and strongest gravitational fields!

→ Tests under extreme conditions

- Nuclear matter
- General relativity & alternatives

[Berti *et al.* (2015)]
[Lattimer, Prakash (2016)]

→ EMT is likely anisotropic

- Relativistic nuclear interactions
- Mixture of fluids of different types
- Presence of superfluid
- Existence of solid core
- Phase transitions
- Presence of magnetic field
- Viscosity
- ...

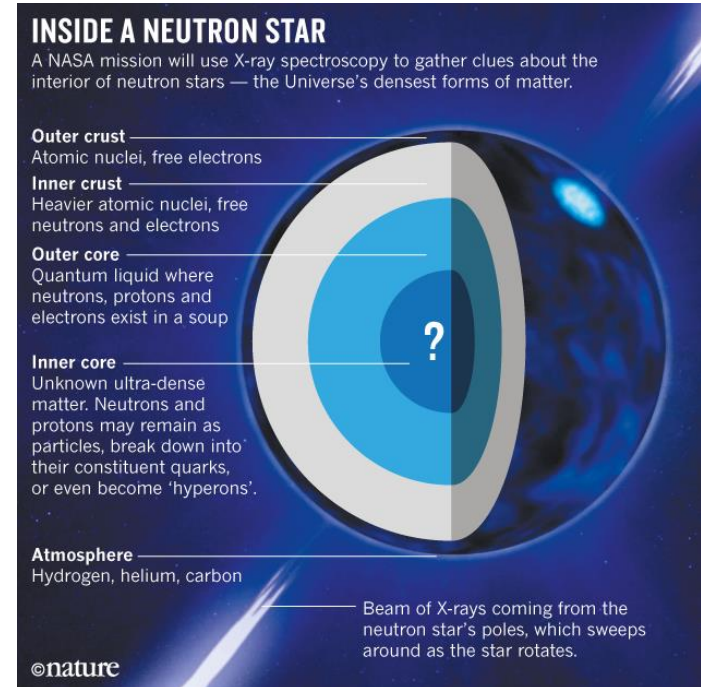
[Ruderman (1972)]
[Canuto (1974)]
[Bowers, Liang (1974)]
[Herrera, Santos (1997)]



$$M_p \sim 1.67 \times 10^{-24} \text{ g}$$

$$R_p \sim 0.84 \text{ fm}$$

$$\rho_p \sim 2.4 \rho_0$$



$$M \sim 1.4 M_{\odot}$$

$$R \sim 10 \text{ km}$$

$$\rho \sim 3 \rho_0$$

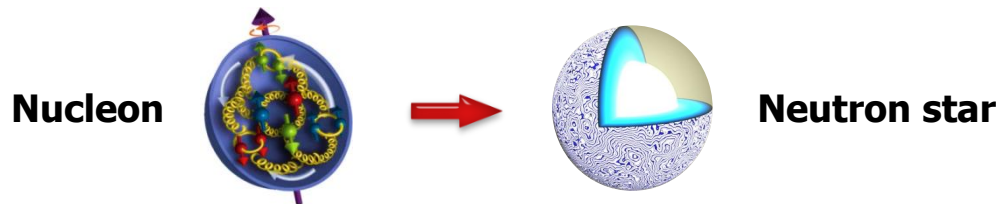
$$g \sim 2.4 \times 10^{12} \text{ m/s}^2$$

$$M_{\odot} = 2 \times 10^{33} \text{ g}$$

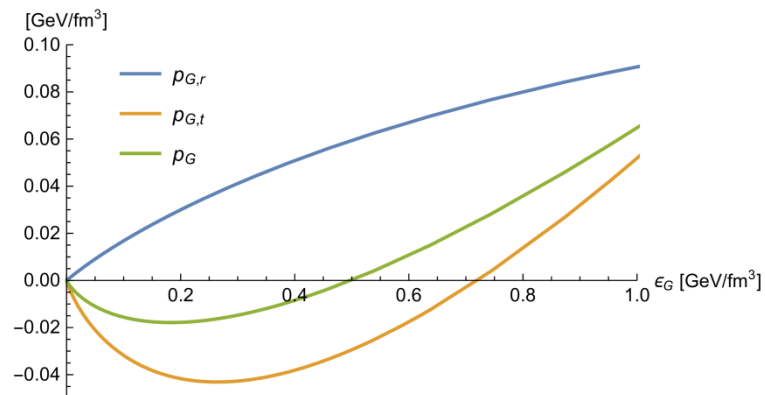
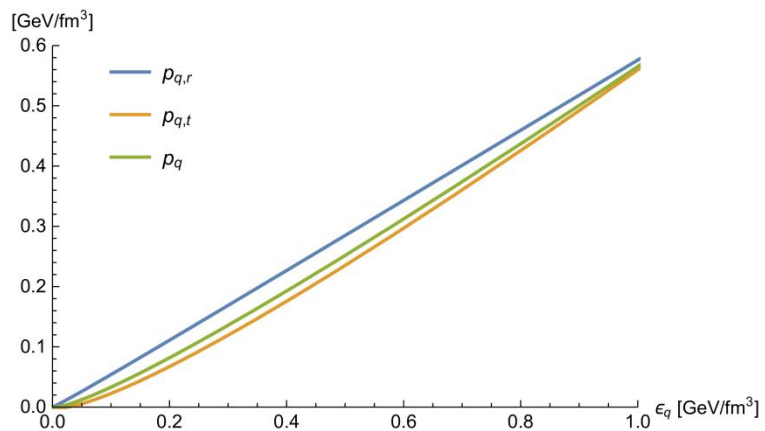
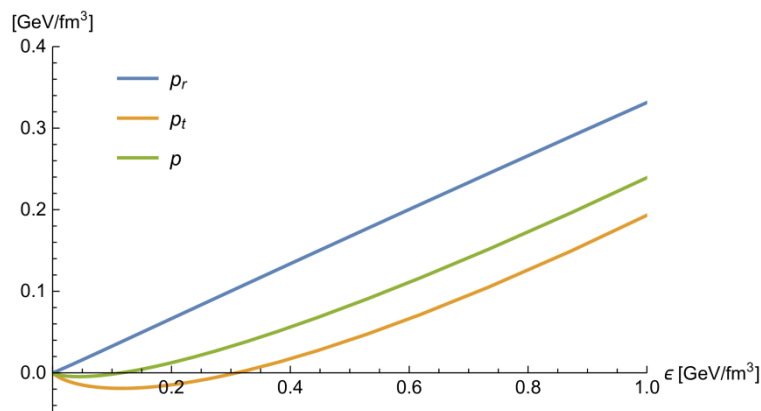
$$\rho_0 = 2.8 \times 10^{14} \text{ g/cm}^3$$

[Potekhin (2010)]

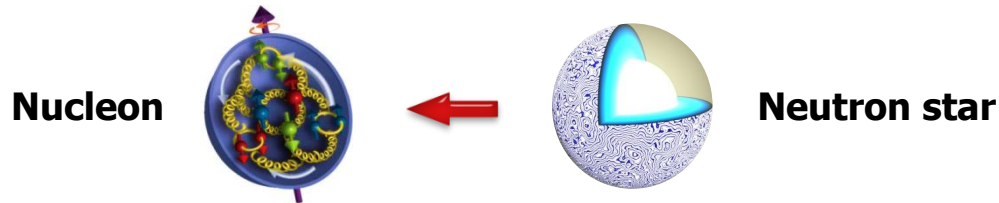
What can we learn?



Equation of state



What can we learn?



Stability constraints

[Wald (1984)]
 [Herrera, Santos (1997)]
 [Poisson (2004)]
 [Abreu, Hernandez, Nunez (2007)]
 [Hawking, Ellis (2011)]

Mechanical regularity

- (i) $\varepsilon(0) < \infty$, $p(0) < \infty$ and $s(0) = 0$;
- (ii) $\varepsilon(r) > 0$ and $p_r(r) > 0$;
- (iii) $\frac{d\varepsilon(r)}{dr} < 0$ and $\frac{dp_r(r)}{dr} < 0$.

Speed of sound

- (iv) $0 \leq v_{sr}^2(r) \leq 1$ and $0 \leq v_{st}^2(r) \leq 1$;
- (v) $|v_{st}^2(r) - v_{sr}^2(r)| \leq 1$;
- (vi) $\Gamma(r) = \frac{\varepsilon(r) + p_r(r)}{p_r(r)} v_{sr}^2 > \frac{4}{3}$.

Energy conditions

$$\begin{aligned} \varepsilon(r) + p_i(r) &\geq 0, \\ \varepsilon(r) + p_i(r) &\geq 0 \quad \text{and} \quad \varepsilon(r) \geq 0, \\ \varepsilon(r) + p_i(r) &\geq 0 \quad \text{and} \quad \varepsilon(r) + 3p(r) \geq 0, \\ \varepsilon(r) &\geq |p_i(r)|, \end{aligned}$$

Summary

- **Mass, spin and pressure** all encoded in EMT

$$T^{\mu\nu} = \begin{bmatrix} T^{00} & T^{01} & T^{02} & T^{03} \\ T^{10} & T^{11} & T^{12} & T^{13} \\ T^{20} & T^{21} & T^{22} & T^{23} \\ T^{30} & T^{31} & T^{32} & T^{33} \end{bmatrix}$$

Energy density: T^{00}
Momentum density: T^{0i}
Energy flux: T^{i0}
Momentum flux: T^{ij}
Shear stress: T^{ij} (off-diagonal)
Normal stress (pressure): T^{ii} (diagonal)

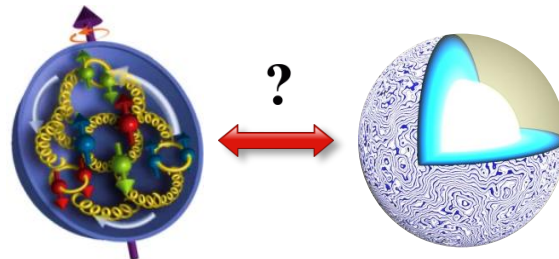
- **Nucleon energy density and pressure are extremely high**

➔ **Large anisotropy**

- **Same ballpark as interior of compact stars**

- **Exciting cross-talk between hadronic physics and neutron star physics!**

➔ **Equation of state, stability constraints, ...**



Backup slides

Gravitational form factors

Mellin moment of twist-2 vector GPDs

$$\langle p', s' | T^{++}(0) | p, s \rangle$$

$$\int dx x H(x, \xi, t) = A(t) + 4\xi^2 C(t)$$

[Ji (1996)]

$$\int dx x E(x, \xi, t) = B(t) - 4\xi^2 C(t)$$

Poincaré covariance

$$\langle p', s' | T_q^{[\alpha\beta]}(0) | p, s \rangle = -i\Delta_\mu \langle p', s' | S_q^{\mu\alpha\beta}(0) | p, s \rangle$$

$$D_q(t) = -G_A^q(t)$$

[C.L., Mantovani, Pasquini (2018)]

EMT trace

$$\langle p', s' | G^2(0) | p, s \rangle, \quad \langle p', s' | \bar{\psi}(0)\psi(0) | p, s \rangle \quad \Rightarrow \quad \bar{C}(t)$$

[Ji (1995)]

[C.L. (2018)]

Recent Lattice QCD results

Mass

[Yang *et al.*, arXiv:1808.08677]

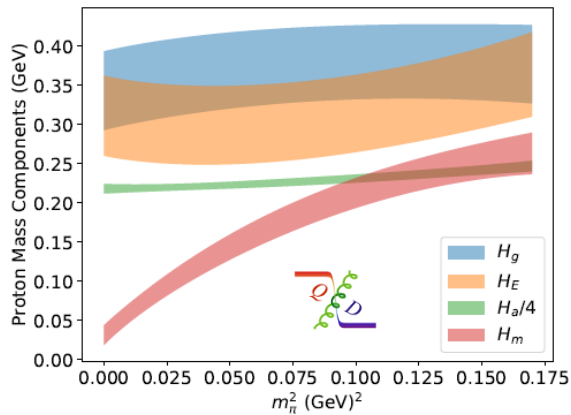


FIG. 3. The valence pion mass dependence of the proton mass decomposition in terms of the quark condensate ($\langle H_m \rangle$), quark energy (H_E), glue field energy (H_g) and trace anomaly (H_a)/4.

Spin

[Alexandrou *et al.*, arXiv:1807.11214]

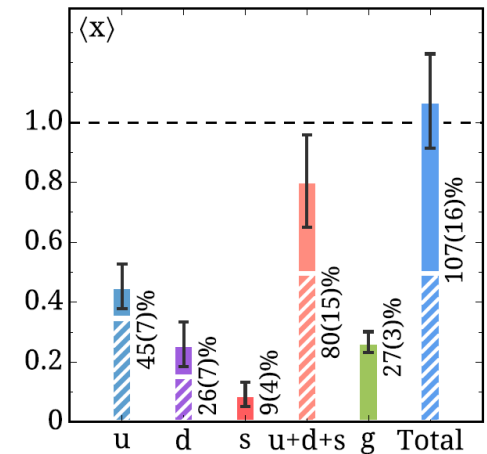
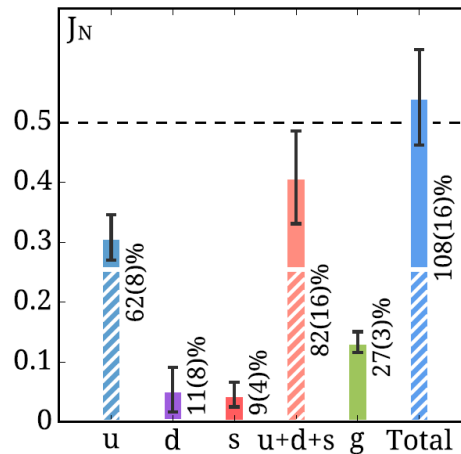


Figure 2: Left: Nucleon spin decomposition. Right: Nucleon momentum decomposition. The striped segments show valence quark contributions (connected) and the solid segments the sea quark and gluon contributions (disconnected). Results are given in $\overline{\text{MS}}$ -scheme at 2 GeV.